Spin-dependent tunneling in semiconductor heterostructures with a magnetic layer

I. V. Rozhansky,[1,2,3,*] K. S. Denisov,[1,2] N. S. Averkiev,[1] I. A. Akimov,[1,4] and E. Lähderanta[2]
[1]*Ioffe Institute, 194021 St. Petersburg, Russia*
[2]*Lappeenranta University of Technology, FI-53851 Lappeenranta, Finland*
[3]*Peter the Great Saint-Petersburg Polytechnic University, 195251 St. Petersburg, Russia*
[4]*Experimentelle Physik 2, Technische Universität, D-44227 Dortmund, Germany*
(Received 6 July 2015; published 21 September 2015)

We present a theory that describes the appearance of circular polarization of the photoluminescence (PL) in ferromagnet-semiconductor hybrid heterostructures due to the spin-dependent tunneling of photoexcited carriers from a quantum well into a magnetic layer. The theory succeeds in explaining the experimental data on time-resolved PL for heterostructures consisting of an InGaAs-based quantum well (QW) and a spatially separated Mn δ layer. We show that the circular polarization of the PL originates from the dynamic spin polarization of electrons due to spin-dependent leakage from the QW onto the Mn donor states split by the exchange field of the ferromagnetic Mn δ layer.

DOI: 10.1103/PhysRevB.92.125428 PACS number(s): 78.20.Ls, 78.67.−n, 75.50.Pp, 75.76.+j

I. INTRODUCTION

The field of semiconductor spintronics can be now claimed as well established. However, the "classical" spintronic devices such as spin transistors [1] or spin valves [2] still do not meet the theoretical expectations to advance modern applied electronics. The key issue yet to be resolved along the way is the fabrication of a good semiconductor with ferromagnetic properties. A substantial breakthrough was the discovery of a (Ga,Mn)As dilute magnetic semiconductor (DMS) [3] with a relatively high Curie temperature of around $T_c \approx 100$ K. So far, the highest Curie temperature achieved for bulk dilute (Ga,Mn)As samples has not exceeded 200 K [4]. While the Mn solubility limit basically prevents a further increase of T_c in bulk samples, hybrid (Ga,Mn)As heterostructures with an Mn layer coupled to a remote two-dimensional (2D) hole channel have gained considerable interest [5–7]. GaAs-based heterostructures with an Mn δ layer located in the vicinity of an $In_xGa_{1-x}As$ quantum well (QW) exhibit a ferromagnetic behavior similar to those of bulk Mn-doped GaAs DMSs. It was demonstrated that the 2D holes populating the QW substantially contribute to the ferromagnetism of the Mn layer due to a resonant indirect exchange interaction [8,9].

The ferromagnetic ordering of the Mn δ layer also gives rise to the circular polarization of the photoluminescence (PL) from the QW. However, the particular microscopic mechanism leading to this phenomenon still is not fully understood. Ferromagnetic (Ga,Mn)As DMSs are p-type semiconductors, so the logical assumption might be that in thermal equilibrium the QW is populated with 2D holes which are spin polarized due to coupling with Mn ions, so that the light emitted from the QW would be circularly polarized. The theory of this mechanism has been developed in Refs. [10,11] and it is probably relevant to the experimental data reported in Refs. [12,13]. However, recent time-resolved experiments on similar samples with more shallow $In_xGa_{1-x}As$ QWs have demonstrated that, under moderate photoexcitation, the spin polarization in GaMnAs-based hybrids is a nonequilibrium, dynamic effect [14].

We argue that in these experiments the circular polarization of the PL stems from the dynamic spin polarization of the photoexcited electrons. This finding does not completely exclude the importance of the holes' spin polarization, but only states the prime role of the dynamic electrons in hybrid structures with a shallow QW (and far less sheet density of the 2D holes that in samples with deeper QWs). In the present paper we provide a theory for the effect which perfectly describes the experimental data. In our model the spin polarization of the electrons remaining in the QW occurs due to an effective spin-dependent tunneling into the magnetic layer, followed by nonradiative recombination. The theoretical description developed appears to be rather general and can be applied to various semiconductor heterostructures with a similar design.

II. MODEL

The band diagram of the system under study is shown schematically in Fig. 1. It consists of an $In_xGa_{1-x}As$ QW sandwiched between GaAs barriers and a thin layer doped with Mn located a few nanometers from the QW. The Mn layer comprises a dilute magnetic semiconductor with a pronounced ferromagnetic behavior. Our theory focuses on the electrons tunneling from the QW into the ferromagnetic Mn layer. The theoretical description developed further is rather general and can be applied to various semiconductor heterostructures with a similar design. However, in the rest of the paper we will concentrate on a particular heterostructure for which a set of experimental data on time-resolved PL has been obtained, allowing for a comparison with theoretical analyses [14,15]. The width of the QW under consideration is $a = 10$ nm and its depth is controlled by In composition. For $x_{In} = 10\%$ the QW depth for the electrons (i.e., the position of the first size quantization level relative to the GaAs conductance band edge) is $W_e = 45$ meV for the temperature $T = 2$ K. The details of the structure design and fabrication can be found in Ref. [13]. The width d of the spacer separating the Mn layer from the QW is varied in the range 2–10 nm for different samples, and

*rozhansky@gmail.com

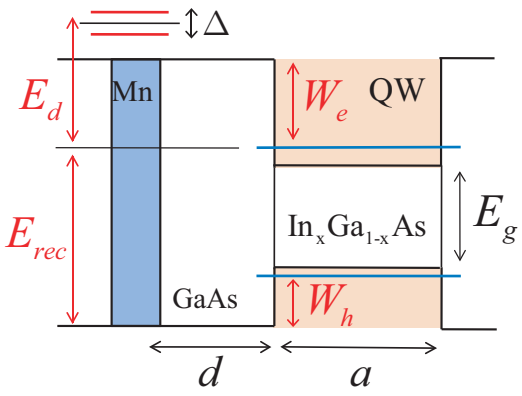

FIG. 1. (Color online) Schematic band structure of the considered ferromagnetic-semiconductor system.

it is penetrable for the electrons as well as for the holes [10]. It is well known that an Mn impurity in a GaAs matrix can exist in two different states. A single Mn atom replacing a Ga atom in the lattice makes an Mn_{Ga} configuration, where Mn behaves as an acceptor with a hole binding energy $E_a \approx 110$ meV. The Mn atom can also occupy an interstitial position Mn_I, at which it becomes a double donor. It has been confirmed experimentally that in the samples under study both Mn_{Ga} and Mn_I configurations are realized [13]. The acceptors Mn_{Ga} provide weakly localized holes mediating the ferromagnetism. The holes are distributed between the Mn doping layer and the QW. It was argued that both fractions can contribute to ferromagnetism, depending on the QW depth [9]. The samples being discussed in this paper had a very shallow QW for the holes ($W_h \approx 30$ meV) so that the tunnel coupling between the Mn layer and the QW is of nonresonant character. Thus, the equilibrium spin polarization of the holes located in the QW is not expected and (along with the kinetics discussed below) cannot fully explain the observed circular polarization of the photoluminescence from the QW. The interstitial Mn_I are known to be effective nonradiative recombination centers [16]. Unlike a Mn_{Ga} substitutional impurity, the Mn_I donors repel positively charged holes and do not directly participate in the hole-mediated ferromagnetism. However, there is a strong antiferromagnetic (AF) superexchange interaction between the Mn ions in an interstitial and a neighboring substitutional position [4,17]. The formation of such Mn_I-Mn_{Ga} pairs is likely as they are more thermally stable than isolated Mn_I [18]. The AF coupling attributed to the neighboring Mn_I-Mn_{Ga} has been observed experimentally [17]. Thus, it is reasonable to assume that while there is a macroscopic magnetization of the sample, not only are Mn_{Ga} spins ferromagnetically aligned, but most of the Mn_I spins are aligned as well (in the opposite direction) [17]. With that taken into account, we conclude that the electron bound states at the Mn_I ions are split in spin projection on the same axis due to an exchange interaction with the core d^5 electrons. Those Mn_I that remain isolated and not coupled to Mn_{Ga} can possibly provide a spin-independent tunneling channel, lowering the degree of dynamic spin polarization discussed below. In our theoretical consideration we will focus only on those Mn_I that are spin split due to AF coupling with the neighboring Mn_{Ga}. Let us consider an electron tunneling from the QW into the spin-split bound state at Mn_I with a subsequent nonradiative recombination with a valence band hole. Taking into account donor level spin splitting, we note that there are two tunneling channels corresponding to opposite electron spin projections. The difference in the tunneling rates for spin-up and spin-down electrons tunneling from the QW to the donor states gives rise to spin polarizations of the electrons remaining in the QW. We argue that this mechanism is responsible for the observed polarization of the PL emitted from the QW.

Let us now proceed to a more detailed theoretical analysis of the phenomena. The exchange interaction between the localized electron and Mn_I core can be expressed as

$$V_{\rm ex} = -\alpha_e \mathbf{JS}, \tag{1}$$

where $\mathbf{J}$ is the Mn_I spin operator, $\mathbf{S}$ is the electron spin operator, and α_e is the exchange coupling constant. The quantity α_e, which describes the s-d exchange, is positive, favoring the ferromagnetic alignment of the donor state electron with the d^5 core electrons. Let E_d be the donor energy level (measured from the size quantization level in the QW, as shown in Fig. 1). Due to the exchange interaction (1) the level is split into two spin sublevels having energies

$$\varepsilon_s = E_d - s\Delta, \quad \Delta = \alpha_e J_z,$$

where s denotes the electron spin projection and J_z is the Mn_I spin projection onto the z axis directed normal to the QW plane. In the external magnetic field applied along the z axis, $B > 0$, the ground state of substitutional Mn_{Ga} corresponds to $-5/2$ spin projection, and thus the Mn_I center has the opposite spin, $J_z = +5/2$. Consequently, the donor state $s = +1/2$ has a lower energy than $s = -1/2$. The position of the donor level energy E_d is quite a delicate question. Experimental data for the Mn_I donor energy level positions are lacking. Theoretical calculations for bulk GaMnAs show the Mn_I donor energy level to be lying in the conductance band [19]. In this case, because of the energy mismatch, there is no direct resonant tunneling from the occupied electron states in the QW onto the spin-split donor level. However, the spin splitting would manifest itself in a second-order process involving the electron tunneling to the donor level, followed by a phonon-assisted nonradiative recombination of the electron with the valence band hole in the Mn layer. The initial state corresponds to a 2D electron in the QW with energy $\varepsilon_k = \hbar^2 k^2/2m$, where k is the 2D wavevector in the plane of the QW, m is the in-plane effective mass, and the final state is the electron in the valence band in the Mn layer and an emitted phonon with energy $\hbar\Omega_q$. We neglect Zeeman splitting for 2D electrons in the QW in comparison with the exchange splitting at the donor site [13]. The matrix element for the electron transition from the QW into the Mn layer is calculated using the second-order perturbation theory. Using the Fermi's golden rule, we get the transition rate

$$d\omega^{\mathbf{q}}_{\mathbf{k},s} = \frac{2\pi}{\hbar}\left|\frac{V_q T}{\varepsilon_k - E_d + s\Delta}\right|^2 \delta(\varepsilon_k + E_{\rm rec} - \hbar\Omega_{\mathbf{q}}) \frac{Sd^2\mathbf{k}d\nu_q}{(2\pi)^2}, \tag{2}$$

where V_q is the electron-phonon interaction matrix element, $d\nu_q$ is the phonon mode density, $E_{\rm rec}$ is the energy difference

between the electron size quantization level in the QW and the top of the valence band in the GaAs barrier (see Fig. 1), T is the tunneling matrix element, and S is the QW area. T depends exponentially on spacer thickness d as $T = \tau e^{-qd}$, where $q = \sqrt{2m_* W_e/\hbar^2}$, m_* is the effective mass of the barrier material in the direction perpendicular to the QW plane, W_e is the electron barrier height (Fig. 1), and the preexponential factor is discussed in Ref. [11]. Integration of (2) over phonon degrees of freedom yields

$$d\omega_{\mathbf{k},s} = \frac{1}{\tau_d}\frac{\tau^2 e^{-2qd}}{(\varepsilon_k - E_d + s\Delta)^2}\frac{Sd^2\mathbf{k}}{(2\pi)^2}, \tag{3}$$

where we introduced the electron lifetime at the donor state

$$\frac{1}{\tau_d} = \frac{2\pi}{\hbar}\int d\nu_{\mathbf{q}}|V_q|^2\delta(E_{\rm rec} - \hbar\Omega_{\mathbf{q}}).$$

The dependence of τ_d on k can be neglected as $\varepsilon_k \ll E_{\rm rec}$. Because the donor level is split, the transition rate (2) appears to be different for opposite spin projections. The nonradiative current density for each spin projection is given by

$$j_s = e\int f_s(\mathbf{k})\frac{d\omega_{\mathbf{k},s}}{S}, \tag{4}$$

where the integration is performed over all 2D states, $f_s(\mathbf{k})$ denotes the thermal distribution function of the electrons in the QW, and e is the electron charge. The electron gas is nondegenerate since the electrons appear in the QW only due to photoexcitation. This implies

$$f_s(\mathbf{k}) = \exp\left(\frac{\mu_s - \varepsilon_k}{k_B T_e}\right), \tag{5}$$

where T_e is the electron temperature, μ_s is the chemical potential for the electrons with s spin projection, and k_B is the Boltzmann constant. The current density for each spin projection (4) is expressed as

$$j_s = e\frac{\tau^2 e^{-2qd}}{\tau_d}\frac{n_s}{k_B T_e}\int_0^\infty \frac{e^{-\varepsilon_k/k_B T_e}}{(\varepsilon_k - E_d + s\Delta)^2}d\varepsilon_k. \tag{6}$$

As there is a large energy mismatch between the electrons in the QW and the donor level, we have $k_B T_e \ll E_d$, so expression (6) can be simplified by setting $\varepsilon_k = 0$ in the denominator, and then the final expression for the current reads

$$j_s = e\gamma_s n_s, \quad \gamma_s = \frac{e^{-2qd}}{\tau_d}\frac{\tau^2}{(E_d - s\Delta)^2}, \tag{7}$$

where n_s is the sheet density of the electrons with s spin projection in the QW, and γ_s is the nonradiative channel recombination rate. Note that while γ_s (7) is reduced by a large value of E_d, the small carrier lifetime at the donor level τ_d can keep the nonradiative current sufficiently high while the perturbation theory still holds. Even with equal sheet densities of the spin-up and spin-down electrons, since $\gamma_{+1/2} \neq \gamma_{-1/2}$, there is a difference between the spin-up and spin-down currents. For $\Delta \ll E_d$ this difference makes

$$j_{+1/2} - j_{-1/2} = en\frac{e^{-2qd}}{\tau_d}\frac{2\tau^2}{E_d^2}\frac{\Delta}{\varepsilon_d}, \tag{8}$$

where n is the electron sheet density in the QW. In a positive external magnetic field $\Delta > 0$, so $j_{+1/2}/e > j_{-1/2}/e$, and the $s = 1/2$ channel is more efficient. This imbalance leads to an accumulation of spin-down electrons in the QW.

III. COMPARISON WITH EXPERIMENT

We applied the model described above to the experimental data on time-resolved PL [14,15]. As the transition rates for spin-up and spin-down electrons leaving the QW through the nonradiative channel are different ($\gamma_{+1/2} \neq \gamma_{-1/2}$), a nonzero spin accumulates in the QW.

The spin polarization of the electrons remaining in the QW gives rise to a circular polarization of the PL from the QW. Let us define the electron spin polarization degree as follows:

$$\rho_s = \frac{n_{+1/2} - n_{-1/2}}{n_{-1/2} + n_{+1/2}}. \tag{9}$$

ρ_s is negative when $s = -1/2$ electrons prevail. In this case the radiative recombination with a heavy hole with an angular momentum projection $j_z = +3/2$ would be more efficient, so the circular polarization σ_+ would dominate in the PL. The sign of the PL circular polarization (which is opposite to the sign of ρ_s as defined above) is an important indicator, confirming the applicability of the suggested spin polarization mechanism to explain the experimental observations. In our model, the nonradiative transition rate is higher for spin-up electrons, so that $\rho_s < 0$ and σ_+ circular polarization dominates in the PL from the QW. This is exactly what is observed in the experiment. Let us now focus on the kinetics of the photoexcited electrons. The characteristic time of nonradiative recombination in (Ga,Mn)As is $\tau_d \sim 1$ ps [16]. However, the electrons leave QW with a characteristic time γ_s^{-1} (7), which is much longer than τ_d. Thus, the electron lifetime in the QW is governed either by the tunneling process or radiative recombination in the QW. Although typically the radiative recombination time $\tau_{\rm rad} \sim 1$ ns is much longer than the nonradiative time γ_s^{-1}, for $d = 10$ nm spacer thickness it becomes comparable to $\gamma_s^{-1} \sim 0.4$ ns. In this case both processes contribute to the total electron recombination rate Γ_s:

$$\Gamma_s = \gamma_s + \tau_{\rm rad}^{-1}.$$

Another process which has a direct influence on ρ_s is carrier spin relaxation. It was found that, in the structures under study, the holes' spin relaxation time is very short, $\tau_s^h \sim 10$ ps [14]. At the same time, the electron spin relaxation time τ_s^e (while increasing with spacer thickness from $\tau_s^e = 1$ ns for $d = 5$ nm to $\tau_s^e = 10$ ns for $d = 10$ nm [14]) is longer than the electron lifetime Γ_s^{-1}.

Let us now consider the PL dynamics in the time-resolved experiment. A short, nonpolarized excitation pulse ($\tau_{\rm pulse} \approx 1$ ps [14]) produces nonequilibrium carriers in the QW. Right after the excitation pulse is switched off, the electron kinetics and PL intensity are governed by radiative recombination and the tunneling. However, since $\Gamma_s^{-1} \ll \tau_s^e$, the spin kinetics and PL polarization are determined only by spin-dependent nonradiative recombination. Assuming immediate energy relaxation, the electron dynamics is described by the following simple expression:

$$\frac{dn_s}{dt} = -j_s/e - \frac{n_s}{\tau_{\rm rad}}.$$

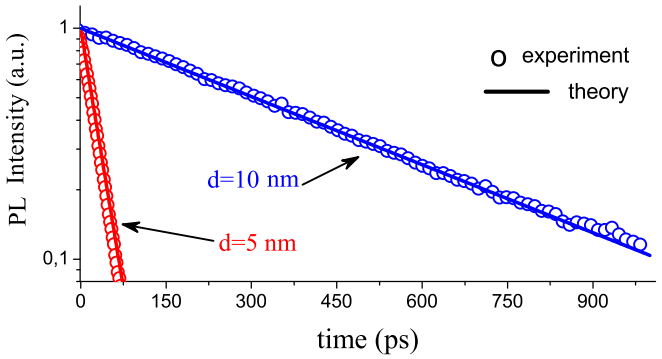

FIG. 2. (Color online) Time dependence of the intensity of the photoluminescence from the QW.

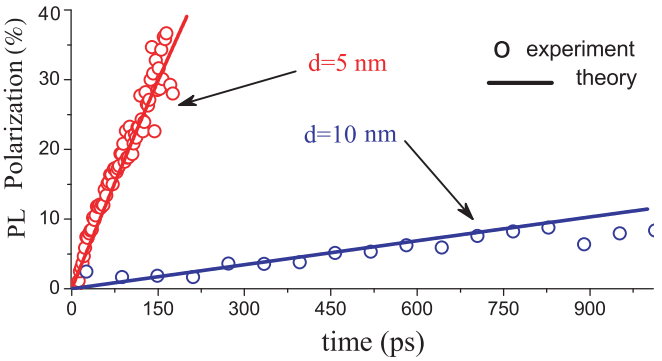

FIG. 3. (Color online) Time dependence of the circular polarization degree of the photoluminescence from the QW.

With j_s given by (7), we get that n_s decays exponentially,

$$n_s = \frac{n_0}{2} e^{-\Gamma_s t},$$

where n_0 is the electron sheet density generated in the QW by the excitation pulse. From the known pulse duration, the upper bound estimate is $n_0 \sim 10^9$ cm^{-2}. Then, the density of the electrons in the QW and the spin polarization degree ρ_s obey

$$n(t) = n_{+1/2} + n_{-1/2} = \frac{n_0}{2}(e^{-\Gamma_{+1/2}t} + e^{-\Gamma_{-1/2}t}),$$
$$\rho_s(t) = \tanh\left(\frac{\delta\Gamma}{2}t\right), \quad \delta\Gamma = \gamma_{+1/2} - \gamma_{-1/2}. \tag{10}$$

Figure 2 shows a comparison of the calculated electron sheet density and spin polarization dynamics (10) with the time dependence of the PL observed in experiments [14,15] for two different spacer thicknesses $d = 5, 10$.

In the calculation we used the following parameters: $\tau = 13$ meV, $\tau_d = 0.5$ ps, $E_d = 47$ meV, $W_e = 45$ meV, $\Delta = 2.5$ meV, and $m_* = 0.065m_0$. Figure 2 shows the PL intensity decreasing with time, following the kinetics of the photoexcited electrons. As noted above, the decay of the PL intensity is very fast compared to the radiative recombination time $\tau_{\rm rad}$. The strong dependence of the PL on the spacer thickness is due to the exponential tunneling factor in (7).

The PL circular polarization degree is shown in Fig. 3. The spin-dependent tunneling ($\delta\Gamma \neq 0$) and long electron spin relaxation time τ_s^e leads to an accumulation of nonequilibrium spin in the QW ρ_s, which increases linearly with time while $t \ll \delta\Gamma^{-1}$ (10). It should be noted that the electron tunneling also leads to an accumulation of positive charge in the QW which might have prevented the tunneling due to an electrostatic effect. However, the value of the positive charge is of the order of the initial electron concentration right after photoexcitation n_0, i.e., no more than $n_0 \sim 10^9$ cm^{-2}, and such a charge density is too small to significantly affect tunneling by electrostatic effects.

IV. SUMMARY

To conclude, we proposed a microscopic mechanism explaining the observed ultrafast PL kinetics and the PL circular polarization in a hybrid ferromagnetic-semiconductor structure with a QW and spatially separated Mn δ layer. The PL behavior in our model is governed by the dynamics of the photoexcited electrons. The key process which determines the electrons' dynamics is their tunneling onto Mn_I interstitial donorlike defects in the Mn layer.

The spin splitting of this donor in the exchange field of the Mn layer makes this tunneling spin dependent and causes an accumulation of nonequilibrium spin in the QW. While the tunneling itself is of a nonresonant character, the leakage of the spin-dependent carriers through the nonradiative channel appears to be effective due to the very small lifetime of a carrier at the donor site. This proposed model allowed us to explain the fast PL decay, the linear increase of the PL circular polarization with time, as well as its sign observed in the experiment.

ACKNOWLEDGMENTS

We thank V. L. Korenev, V. F. Sapega, and S. V. Zaitsev for very fruitful discussions. This work was supported by the Government of Russia through the program P220 (Project No. 14.Z50.31.0021, led by M. Bayer), RF President Grant NSh-1085.2014.2. K.S.D. acknowledges the support of the Dynasty Foundation.

[1] S. Datta and B. Das, Appl. Phys. Lett. **56**, 665 (1990).
[2] R. Jansen, J. Phys. D: Appl. Phys. **36**, R289 (2003).
[3] H. Ohno, A. Shen, F. Matsukura, A. Oiwa, A. Endo, S. Katsumoto, and Y. Iye, Appl. Phys. Lett. **69**, 363 (1996).
[4] T. Dietl and H. Ohno, Rev. Mod. Phys. **86**, 187 (2014).
[5] B. Rupprecht, W. Krenner, U. Wurstbauer, C. Heyn, T. Windisch, M. A. Wilde, W. Wegscheider, and D. Grundler, J. Appl. Phys. **107**, 093711 (2010).
[6] Y. Nishitani, D. Chiba, M. Endo, M. Sawicki, F. Matsukura, T. Dietl, and H. Ohno, Phys. Rev. B **81**, 045208 (2010).
[7] B. A. Aronzon, M. A. Pankov, V. V. Rylkov, E. Z. Meilikhov, A. S. Lagutin, E. M. Pashaev, M. A. Chuev, V. V. Kvardakov, I. A. Likhachev, O. V. Vihrova *et al.*, J. Appl. Phys. **107**, 023905 (2010).
[8] I. V. Rozhansky, N. S. Averkiev, I. V. Krainov, and E. Lahderanta, Phys. Status Solidi A **211**, 1048 (2014).

[9] I. V. Rozhansky, I. V. Krainov, N. S. Averkiev, B. A. Aronzon, A. B. Davydov, K. I. Kugel, V. Tripathi, and E. Lahderanta, Appl. Phys. Lett. **106**, 252402 (2015).
[10] I. V. Rozhansky, I. V. Krainov, N. S. Averkiev, and E. Lähderanta, Phys. Rev. B **88**, 155326 (2013).
[11] I. V. Rozhansky, N. S. Averkiev, and E. Lähderanta, Low Temp. Phys. **39**, 28 (2013).
[12] V. I. Okulov, A. T. Lonchakov, T. E. Govorkova, K. A. Okulova, S. M. Podgornykh, L. D. Paranchich, and S. Y. Paranchich, Low Temp. Phys. **37**, 220 (2011).
[13] S. Zaitsev, M. Dorokhin, A. Brichkin, O. Vikhrova, Y. Danilov, B. Zvonkov, and V. Kulakovskii, JETP Lett. **90**, 658 (2010).
[14] V. Korenev, I. Akimov, S. Zaitsev, V. Sapega, L. Langer, D. Yakovlev, Y. A. Danilov, and M. Bayer, Nat. Commun. **3**, 959 (2012).
[15] I. Akimov, V. L. Korenev, V. F. Sapega, L. Langer, S. V. Zaitsev, Y. A. Danilov, D. R. Yakovlev, and M. Bayer, Phys. Status Solidi B **251**, 1663 (2014).
[16] H. Nemec, A. Pashkin, P. Kuzel, M. Khazan, S. Schnull, and I. Wilke, J. Appl. Phys. **90**, 1303 (2001).
[17] Y. Takeda, M. Kobayashi, T. Okane, T. Ohkochi, J. Okamoto, Y. Saitoh, K. Kobayashi, H. Yamagami, A. Fujimori, A. Tanaka *et al.*, Phys. Rev. Lett. **100**, 247202 (2008).
[18] T. A. L. Lima, U. Wahl, V. Augustyns, D. J. Silva, A. Costa, K. Houben, K. W. Edmonds, B. L. Gallagher, R. P. Campion, M. J. Van Bael *et al.*, Appl. Phys. Lett. **106**, 012406 (2015).
[19] P. Mahadevan and A. Zunger, Phys. Rev. B **68**, 075202 (2003).